0026-895X/05/6803-690–700$20.00
MOLECULAR PHARMACOLOGY
Copyright © 2005 The American Society for Pharmacology and Experimental Therapeutics
Mol Pharmacol 68:690–700, 2005

Vol. 68, No. 3
12898/3050588
Printed in U.S.A.

HIV Protease Inhibitors Activate the Unfolded Protein Response in Macrophages: Implication for Atherosclerosis and Cardiovascular Disease

Huiping Zhou, William M. Pandak, Jr., Vijay Lyall, Ramesh Natarajan, and Phillip B. Hylemon

Department of Microbiology & Immunology (H.Z., P.B.H.), Division of Gastroenterology, Department of Internal Medicine and McGuire Veterans Affairs Medical Center (W.M.P.), Department of Physiology (V.L.), and Division of Pulmonary and Critical Care Medicine, Department of Internal Medicine (R.N.), Virginia Commonwealth University, Richmond, Virginia

Received March 16, 2005; accepted June 23, 2005

ABSTRACT

Human immunodeficiency virus (HIV) protease inhibitors have been successfully used in highly active antiretroviral therapy for HIV-1 infection. Treatment of patients infected with HIV with HIV protease inhibitors is unfortunately associated with a number of clinically significant metabolic abnormalities and an increased risk of premature atherosclerosis and myocardial infarction. However, the cellular/ molecular mechanisms of the HIV protease inhibitor-induced lipid dysregulation and atherosclerosis remain elusive. Macrophages are the most prominent cell type present in atherosclerotic lesions and play essential roles in both early lesion development and late lesion complications. In this study, we demonstrate that three different HIV protease inhibitors (ritonavir, indinavir, and atazanavir) induce endoplasmic reticulum stress and activate the unfolded protein response in mouse macrophages. Furthermore, at therapeutic concentrations (5–15 μM), these HIV protease inhibitors were found to increase the levels of transcriptionally active sterol regulatory element binding proteins, decrease endogenous cholesterol esterification, cause the accumulation of free cholesterol in intracellular membranes, deplete endoplasmic reticulum calcium stores, activate caspase-12, and increase apoptosis in macrophages. These findings provide possible cellular mechanisms by which HIV protease inhibitors promote atherosclerosis and cardiovascular disease in HIV-1 infected patients treated with HIV protease inhibitors.

HIV protease inhibitors (PIs) have been successfully used in highly active antiretroviral therapy (HAART) for HIV-1 infection and is the most effective treatment currently available. Incorporation of PIs in HAART has significantly reduced the morbidity and mortality and prolonged the lifespan of patients with HIV infection. The benefits of HIV PIs are unfortunately compromised by a number of clinically significant adverse side effects (Hui, 2003). Most patients on HAART develop hyperlipidemia, lipodystrophy, and insulin resistance (Carr et al., 1998; Koster et al., 2003; Beregszaszi et al., 2003; Bongiovanni et al., 2004). Moreover, HAART significantly increases the risk of premature atherosclerosis and myocardial infarction (Holmberg et al., 2004). Recent studies suggest that PIs disrupt cellular lipid homeostasis by increasing the levels of transcriptionally active sterol regulatory element-binding proteins (SREBPs) (Riddle et al., 2001; Williams et al., 2004), endoplasmic reticulum (ER) membrane-bound transcription factors that when proteolytically activated increase the expression of dozens of genes involved in lipid metabolism (Horton et al., 2002). However, the cellular/molecular mechanisms underlying the HIV PI-associated metabolic abnormalities remain elusive and maybe multifactorial.

The unfolded protein response (UPR) is an intracellular signaling pathway, which uses unique regulatory mechanisms to cope with the accumulation of unfolded or misfolded proteins in the ER and plays an important role in regulating cell growth, differentiation, and apoptosis (Oyadomari and

This work was supported by National Institutes of Health grants R01-AI057189 and P01-DK38030.
Article, publication date, and citation information can be found at http://molpharm.aspetjournals.org.
doi:10.1124/mol.105.012898.

ABBREVIATIONS: HIV, human immunodeficiency virus; PI, protease inhibitor; HAART, highly active antiretroviral therapy; SREBP, sterol regulatory element-binding protein; ER, endoplasmic reticulum; UPR, unfolded protein response; AM, acetoxymethyl ester; LDLR, low-density lipoprotein receptor; LDL, low-density lipoprotein; Ac-LDL, acetylated low-density lipoprotein; FBS, fetal bovine serum; PBS, phosphate-buffered saline; CHOP, C/EBP homologous protein; DMEM, Dulbecco's modified Eagle's medium; FITC, fluorescein isothiocyanate; HBSS, HEPES-buffered saline solution; XBP-1, X-box-binding protein 1; ATF, activating transcription factor.

Mori, 2004; Zhang and Kaufman, 2004). Several UPR components have been identified in mammalian cells, which include three transducers [ER transmembrane kinase/endoribonuclease IRE1, doubled-stranded RNA-activated protein kinase-like ER kinase, and activating transcription factor 6 (ATF-6)] and one master regulator [an ER chaperone protein (BiP/GRP78; Zhang and Kaufman, 2004)]. Under various physiological and pathological conditions, the protein folding in the ER is impaired, which causes ER stress. Many ER stress inducers may activate the UPR: accumulation of misfolded proteins, inhibition of N-linked glycosylation, depletion of ER calcium stores, glucose deprivation, redox status, and accumulation of free cholesterol in the ER (Feng et al., 2003; Rutkowski and Kaufman, 2004). Although an elicited response aids the cell in surviving stress, prolonged activation of the UPR ultimately leads to programmed cell death.

Macrophages are the most prominent cell type present in atherosclerotic lesions and play essential roles in all phases of atherosclerosis (Tabas, 2004). It has been demonstrated recently that accumulation of excess free cholesterol in the ER can activate the UPR and induce apoptosis in macrophages (Feng et al., 2003). In the present study, we examined the effects of different HIV PIs on lipid metabolism and the UPR activation in macrophages. The results show that HIV PIs increased levels of transcriptionally active SREBPs, induced accumulation of intracellular free cholesterol, decreased ER calcium stores, activated the UPR, and significantly increased apoptosis in macrophages. These results provide novel insights into the cellular mechanisms whereby HIV PIs induce lipid dysregulation and accelerate atherosclerosis.

Materials and Methods

Materials. Mouse J774A.1 macrophage cells were purchased from American Type Culture Collection (Manassas, VA). Cell culture reagents and NuPAGE Novex Bis-Tris and Tris-acetate Gels were obtained from Invitrogen (Carlsbad, CA). Fetal bovine serum was from Atlanta Biologicals (Norcross, GA) and was heat-inactivated for 30 min at 65°C. Lipoprotein-deficient bovine calf serum was from Biomedical Technologies Inc. (Stoughton, MA). Antibodies against C/EBP-homologous protein (CHOP), activating transcription factor 4 (ATF-4), X-box-binding protein 1 (XBP-1), Lamin B, SREBP-1, and SREBP-2 and horseradish peroxidase-conjugated donkey anti-goat IgG were from Santa Cruz Biotechnology (Santa Cruz, CA). Bio-Rad protein assay reagent, horseradish peroxidase-conjugated goat anti-rabbit IgG, and Precision Plus Protein Kaleidoscope Standards were from Bio-Rad (Hercules, CA). BD ApoAlert Annexin V kit was from BD Biosciences (Palo Alto, CA). Antifade mounting solution and Fura-2 AM were from Molecular Probes (Eugene, OR). SIL 1 B gel plates were from J.T. Baker (Phillipsburg, NJ). [^{3}H]Oleate and [^{14}C]cholesteryl oleate were from PerkinElmer Life and Analytical Sciences (Boston, MA). Ritonavir, indinavir, and atazanavir were generous gifts from Abbott Laboratories (Abbott Park, IL), Merck & Co., Inc. (Whitehouse Station, NJ), and Bristol-Meyers-Squibb (New Brunswick, NJ). BioMax MS film was obtained from Eastman Kodak (Rochester, NY). Concanavalin A was purchased from Biomeda (Foster City, CA). Caspase-12 Fluorometric assay kit was from BioVision (Mountain View, CA). Free Cholesterol C and Cholesterol E assay kits were from Wako Bioproducts (Richmond, VA). RNAqueous total RNA isolation kit was from Ambion (Austin, TX). High-Capacity cDNA archive kit and gene expression kits for mouse ATP-binding cassette (ABC) A1, ABCG1, CD36, and mouse LDL receptor (LDLR) were from Applied Biosystems (Foster City, CA). Modified human lipoprotein acetylated LDL (Ac-LDL) was from Intracel (Frederick, MD). All chemical reagents, including filipin III and Oil Red O, were from Sigma (St Louis, MO). C57BL/6 male mice were from Harlan Bioproducts for Science Inc. (Indianapolis, IN).

Cell Culture and HIV PI Treatment. Mouse J774A.1 macrophages were maintained in DMEM supplemented with 10% FBS, 100 U/ml penicillin, and 100 μg/ml streptomycin at 37°C with 5% CO_2. Cells from passages six to nine were used in these studies. Ritonavir and atazanavir were dissolved in ethanol. Indinavir was dissolved in H_2O. HIV PIs were directly added to culture medium (final concentration, 5 to 50 μM) and incubated for 0.5 to 24 h.

Isolation of Mouse Peritoneal Macrophages. Adult male C57BL/6 mice were injected intraperitoneally with 0.5 ml of phosphate-buffered saline (PBS) containing 40 μg of concanavalin A. The macrophages were harvested 72 h after injection by peritoneal lavage. The harvested cells were cultured in DMEM containing 10% fetal bovine serum (FBS) and 20% L-cell–conditioned medium (Stanley et al., 1976; Koster et al., 2003). The medium was replaced every 24 h until the macrophages were confluent.

Filipin Staining of Free Cholesterol. Mouse J774A.1 macrophages were plated on 22 × 22-mm glass cover slips in six-well plates. The medium was replaced after 24 h, and cells were treated with control vehicle, HIV PIs (5–50 μM), or thapsigargin (100 nM) for 24 h. The cells were fixed with 3.7% formaldehyde in PBS for 10 min and permeabilized with 0.1% Triton X-100 in PBS for 3 min at 4°C. After washing with PBS, the cells were stained with filipin (50 μg/ml) dissolved in PBS containing 0.5% BSA for 30 min at 37°C followed by extensive washing with PBS. The coverslips were mounted onto glass slides using antifade mounting solution. The filipin-free cholesterol complexes were visualized by fluorescence microscopy using Olympus epifluorescence microscope with excitation at 380/40 nm and emission at 485/35 nm.

Measurement of Intracellular Free Cholesterol and Cholesterol Ester. Mouse J774A.1 macrophages were plated on 100-mm plates. The medium was replaced after 24 h, and cells were treated with control vehicle, HIV PIs (5–25 μM), or thapsigargin (100 nM) for 24 h. The cells were collected and washed with PBS. The intracellular total and free cholesterol were measured by using Wako Cholesterol E and Free Cholesterol assay kits (Wako Bioproducts). The amount of cholesterol ester was calculated by subtracting free cholesterol from total cholesterol.

Western Blot Analysis. The nuclear extract was isolated from cells as described previously (Williams et al., 2004). The protein concentration was determined using Bio-Rad protein assay reagent. The nuclear extract (15 μg of protein) was resolved on 10% Bis-Tris or 7% Tris-Acetate NuPAGE Novex gels and transferred to Nitrocellulose membranes. Immunoblots were blocked overnight at 4°C with 5% nonfat milk in Tris-buffered saline and incubated with antibodies to CHOP, XBP-1, ATF-4, SREBP-1, SREBP-2, or lamin B. Immunoreactive bands were detected using horseradish peroxidase–conjugated secondary antibody and the Western Lightning Chemiluminescence reagent plus. The density of immunoblot was analyzed using Image J computer software (http://rsb.info.nih.gov/ij/).

Cholesterol Esterification Assay. Mouse J774A.1 macrophages were plated in DMEM containing 10% FBS for 24 h. Media were replaced with DMEM containing 10% lipoprotein-deficient bovine calf serum. Cells were treated with ritonavir (15 or 25 μM) or control vehicle for 24 h in the presence (20 μg/ml) or absence of LDL and pulsed with [^{3}H]oleate (2 Ci/ml) for 2 h. The lipids were extracted with hexane/isopropyl alcohol [3:2 (v/v)] as described previously (Williams et al., 2004). A recovery standard (30 μg of cholesteryl oleate, 30 μg of triolein, and 0.0005 μCi of [^{14}C]cholesteryl oleate) was added. The extracted samples were dried under a nitrogen gas atmosphere. The lipids were separated by thin-layer chromatography using heptane/ethyl ether/acetic acid [90:30:1 (v/v/v)] and visualized by iodine. The [^{3}H]cholesteryl oleate was quantified by liquid scintillation spectrometry.

Analysis of Apoptosis by Annexin V and Propidium Iodine Staining. Mouse J774A.1 macrophages were treated with various concentrations of ritonavir for 24 h and stained with Annexin V and propidium iodide using BD ApoAlert Annexin V kit according to the protocol recommended by the manufacturer. Annexin V/propidium iodide-stained cells were visualized under confocal fluorescence microscope with a 40× oil immersion objective using a dual filter set for FITC and rhodamine. Cells stained with Annexin V and propidium iodide were further analyzed by two-color flow cytometry to quantify the apoptotic cells. Annexin V and propidium iodide emissions were detected in the FL1 and FL2 channels of a Cytomics FC 500 flow cytometer (Beckman Coulter, Fullerton, CA). At least 10,000 cells were analyzed in each experiment.

Measurement of Caspase-12 Activity. Mouse J774A.1 macrophages were treated with various concentrations of ritonavir or thapsigargin (100 nM) for 24 h. The total cell lysate was prepared. The caspase-12 activity was measured by using Caspase-12 fluorometric assay kit according to the manufacturer instruction (BioVision).

Assay of Endoplasmic Reticulum Calcium Pools. Mouse J774A.1 macrophages were grown on 22 × 40-mm coverslips and treated with vehicle or ritonavir for 24 h. The cells were loaded with 4 μM Fura-2 AM and 0.3% Plurinic F-127 in HBSS at 37°C for 60 min and incubated in HBSS for additional 30 min, then mounted on the stage of an Axioskop 2 plus upright fluorescence microscope (Carl Zeiss GmbH, Jena, Germany) equipped with a 40× objective. After washing with HBSS without Ca^{2+} and Mg^{2+} for three times, the cells were stimulated with 100 nM thapsigargin. Fluorescence images (510-nm emission after alternate 340- and 380-nm excitation) before and after addition of thapsigargin were collected at 15-s intervals through a cooled charge-coupled device camera (TILL Photonics LLC, Martinsreid, Germany) which is attached to an image intensifier (VS4–1845; Videoscope, Washington, DC), an epifluorescent light source (Polychrome IV; TILL Photonics), a 515 nm dichroic beam splitter, and a 535 nm emission filter (20 nm band pass; Omega Optical, Brattleboro, VT). The 340:380 ratios of individual cells in these images were analyzed using TILLvisION version 3.1 imaging software.

RNA Isolation and Real-time Quantitative PCR. Total cellular RNA was isolated from mouse J774A.1 macrophages after treatment with ritonavir (15 μM), thapsigargin (100 nM), or vehicle control for 24 h, using an Ambion RNAqueous kit. Total RNA (10 μg) was used for first-strand cDNA synthesis using High-Capacity cDNA archive kit (Applied Biosystems). The mRNA levels of ABCA1, ABCG1, CD36, and LDLR were quantified using the specific gene expression assay kits for mouse ABCA1, ABCG1, CD36, and LDLR on an ABI PRISM 7700 Sequence Detection System. The mRNA values for each gene were normalized to internal control β-actin mRNA. The ratio of normalized mean value for each treatment groups to vehicle control was calculated.

Oil Red O Staining. Mouse J774A.1 macrophages were plated on 22 × 22-mm glass coverslips in six-well plates. The medium was replaced after 24 h. Cells were loaded with Ac-LDL (50 μg/ml) or vehicle control for 24 h then treated with ritonavir (15 μM), thapsigargin (100 nM), or vehicle control for 24 h. Cells were fixed with 3.7% formaldehyde in PBS for 30 min followed by two washes with PBS. The cells were stained with 0.2% Oil Red O in 60% 2-propanol for 10 min and washed with three times with PBS. The images were taken with the use of a microscope (Olympus, Tokyo, Japan) equipped with image recorder under 40× lenses.

Statistical Methods. Student's t test was employed to analyze the differences between sets of data. Statistics were performed using Prism 4 (GraphPad, San Diego, CA).

Results

HIV PIs Activate the UPR and Induce Apoptosis in Macrophages. We initially examined the effects of HIV PIs on activation of the UPR in cultured mouse J774A.1 macrophages. Induction of the downstream transcription factors, XBP-1, ATF-4, and CHOP are markers for activation of the UPR. Treatment of mouse macrophages with therapeutically relevant concentrations (5–15 μM) of PIs significantly in-

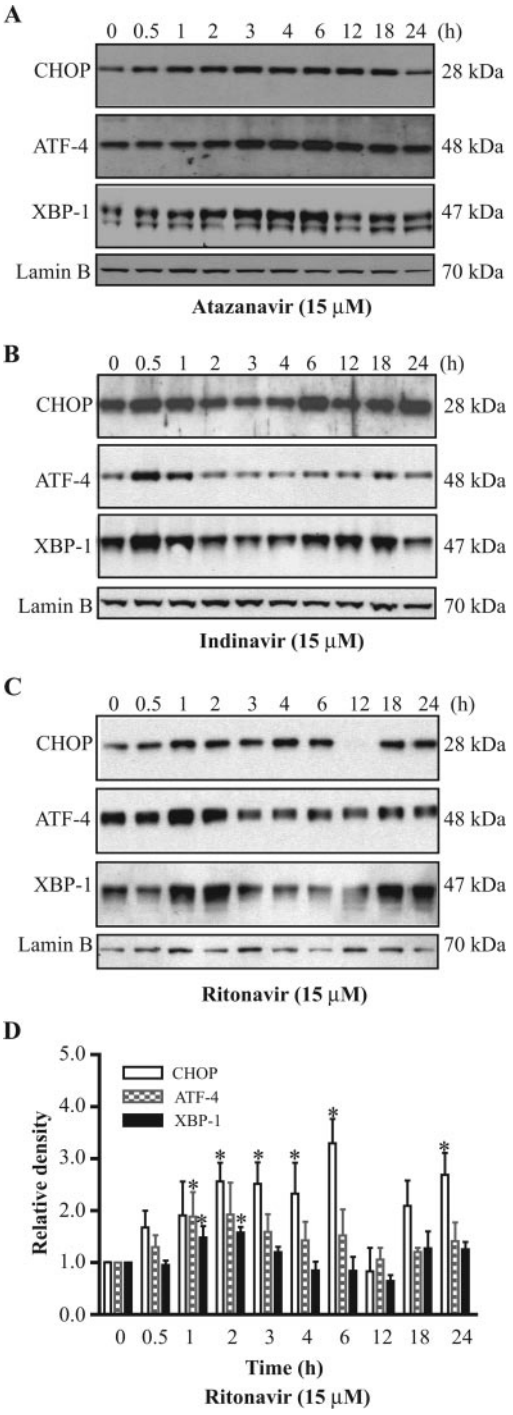

Fig. 1. Activation of the UPR by HIV PIs. Representative immunoblots against CHOP, ATF-4, XBP-1, and lamin B from the nuclear extracts of mouse J774A.1 macrophages treated with HIV PIs (15 μM) for 0, 0.5, 1, 2, 3, 4, 6, 12, 18, and 24 h. Lamin B was used as a loading control. Atazanavir (A), indinavir (B), ritonavir (C), relative density of the immunoblots against CHOP, ATF-4, and XBP-1 activated by ritonavir (D). The density of the immunoreactive bands was analyzed using Image J software and normalized to lamin B control. Values are mean ± S.E. of three independent experiments. *, statistical significance relative to vehicle control, $p < 0.05$.

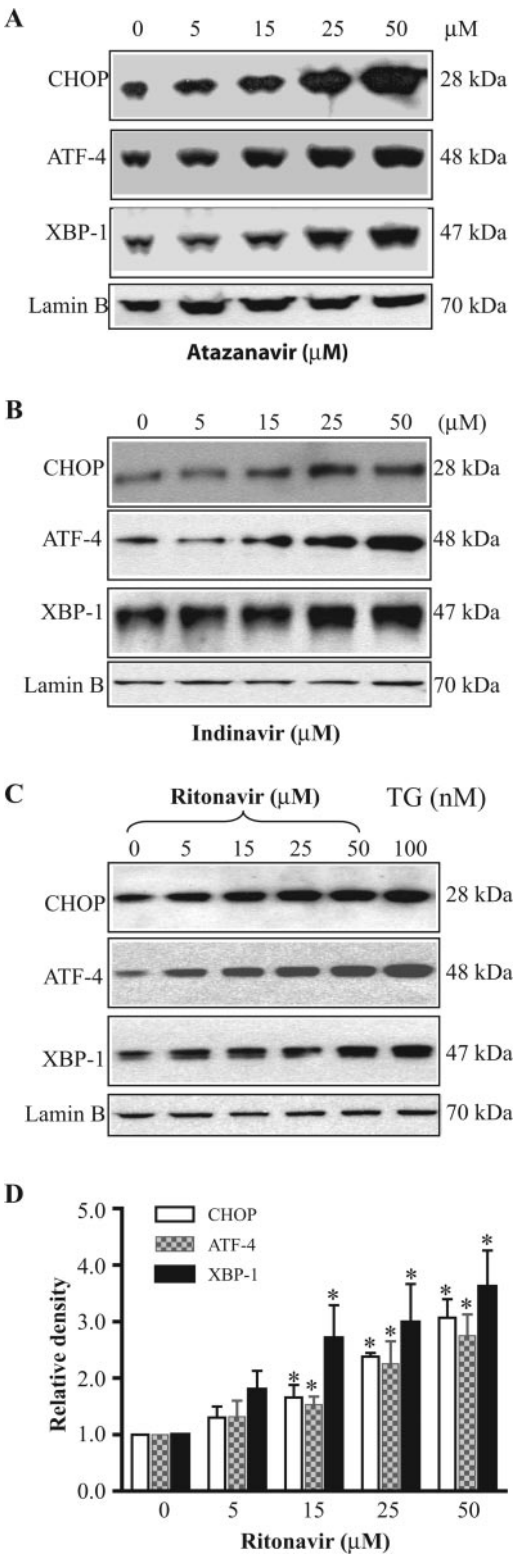

Fig. 2. Concentration-dependent activation of the UPR by HIV PIs in macrophages. Representative immunoblots against CHOP, ATF-4, XBP-1, and lamin B from the nuclear extracts of mouse J774A.1 macrophages treated with the different concentrations of atazanavir (A), indinavir (B), ritonavir (C) (0–50 μM), or thapsigargin (100 nM) for 3 h. Thapsigargin, a known inducer of CHOP, ATF-4, and the UPR, is shown for control purposes. Lamin B was used as a loading control. D, relative density of the immunoblots against CHOP, ATF-4, and XBP-1 activated by ritonavir. The density of the immunoreactive bands was analyzed using Image J software and normalized to lamin B control. Values are mean ± S.E. of three independent experiments. *, statistical significance relative to vehicle control, $p < 0.05$.

creased the expression of CHOP, ATF-4, and XBP-1 (Fig. 1). The expression levels of CHOP, ATF-4, and XBP-1 induced by atazanavir all peaked at 6 h (Fig. 1A). The indinavir-induced activation of CHOP, ATF-4, and XBP-1 peaked at 6, 0.5, and 0.5 h, respectively (Fig. 1B). The expression levels of CHOP, ATF-4, and XBP-1 induced by ritonavir peaked at 6, 1, and 2 h, respectively (Fig. 1, C and D). As shown in Fig. 2, the HIV PI-induced activation of these transcription factors was concentration-dependent. At 15 μM, ritonavir increased the expression of CHOP, ATF-4, and XBP-1 by 66, 53, and 170%, respectively, after a 3-h treatment.

To further confirm that the HIV PI-induced activation of the UPR was not a phenomenon of cultured macrophages, we isolated primary mouse peritoneal macrophages. Treatment (3 h) of these cells with HIV PIs also markedly activated the UPR. The expression of CHOP was increased by 240, 144, and 140% after treatment with ritonavir, indinavir and atazanavir (15 μM), respectively (Fig. 3).

CHOP is one of the most inducible genes during ER stress and is involved in ER stress-induced apoptosis. When mouse J774A.1 macrophages were treated with ritonavir (5–50 μM) for 24 h, morphological changes characteristic of apoptosis were observed (Fig. 4A). To quantify the apoptotic or necrotic cells induced by ritonavir, mouse macrophages were treated with drug for 24 h, stained with Annexin V and propidium iodide, and analyzed by flow cytometry. As shown in Fig. 4B, treatment with ritonavir resulted in a concentration-dependent increase in apoptotic cells. The percentages of apoptotic cells were increased by 17% and 30%, respectively, after treatment with 5 and 15 μM ritonavir for 24 h. Indinavir and atazanavir also induced apoptosis in macrophages (data not shown).

Caspases are cysteine proteases involved in programmed cell death. More than a dozen different caspases have been identified so far. It has been demonstrated that caspase-12 is predominantly associated with the ER and is believed to mediate an ER-specific apoptotic pathway (Nakagawa et al., 2000). Treatment of mouse macrophages with ritonavir (5–25 μM) significantly activated caspase-12. At a concentration of 15 μM, caspase-12 activity was increased by 1.9-fold (Fig. 4C).

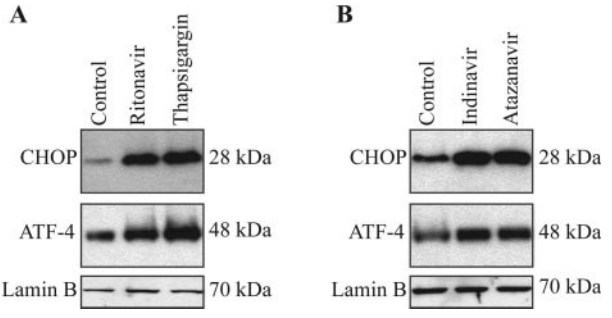

Fig. 3. HIV PIs activate the UPR in primary mouse peritoneal macrophages. A, ritonavir induced activation of the UPR. Representative immunoblots against CHOP, ATF-4, and lamin B from the nuclear extracts of mouse peritoneal macrophages treated with ritonavir (15 μM) or thapsigargin (100 nM) for 3 h. Thapsigargin, a known inducer of CHOP, ATF-4, and the UPR, is shown for control purposes. Lamin B was used as a loading control. B, indinavir and atazanavir induced activation of the UPR. Representative immunoblots against CHOP, ATF-4, and lamin B from the nuclear extracts of mouse peritoneal macrophages treated with indinavir (15 μM) or atazanavir (15 μM) for 3 h. Lamin B was used as a loading control.

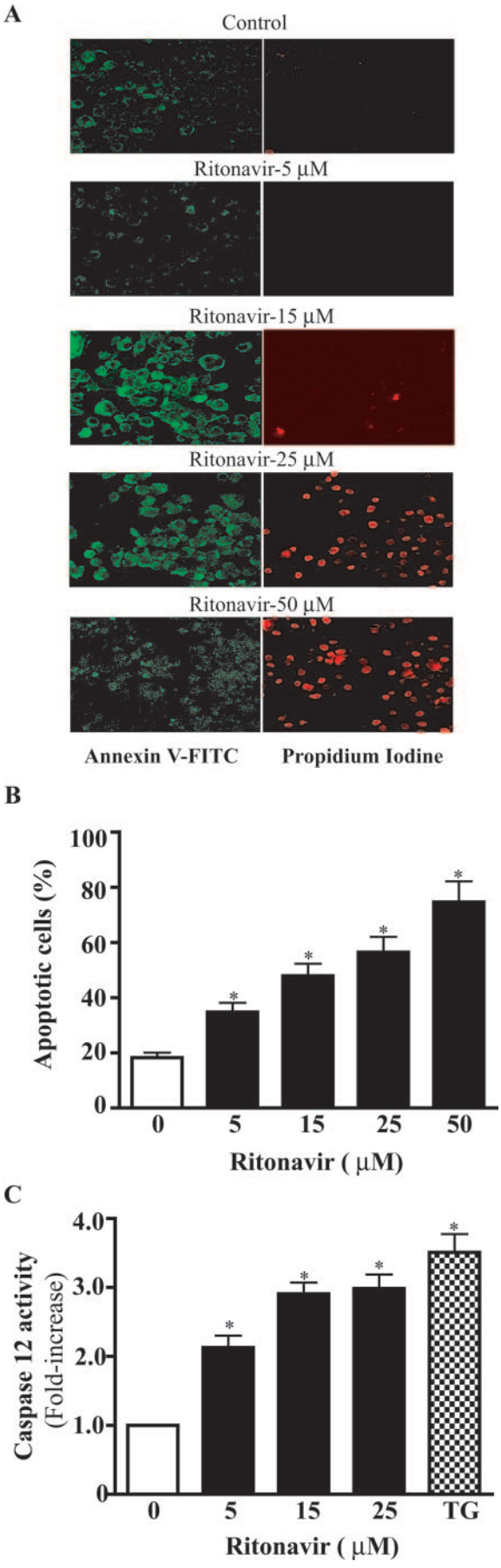

Depletion of ER Calcium Stores by HIV PIs. The ER is a principal site of the synthesis for protein, sterols, cholesterol, and other lipids. Maintenance of ER calcium homeostasis is essential for many cellular functions. Perturbation of ER calcium homeostasis is expected to induce the ER stress. Thapsigargin (a sarcoplasmic/ER calcium-ATPase inhibitor) depletes the ER calcium stores and activates the UPR in many different cells (Yamaguchi and Wang, 2004). To investigate the possible mechanisms of the HIV PI-induced ER stress and activation of the UPR, we assessed the effect of ritonavir on ER calcium stores in mouse J774A.1 macrophages with the fluorescent calcium indicator fura-2/AM. After treatment with different concentrations of ritonavir for 24 h, cells were loaded with fura-2/AM and switched to calcium-free medium. ER calcium release induced by 100 nM thapsigargin was recorded by fluorescence microscopy. Treatment of mouse J774A.1 macrophage with ritonavir decreased the ER calcium content in a dose-dependent manner (Fig. 5). Cells treated with 25 μM ritonavir remarkably reduced the response to thapsigargin, indicating that ER calcium stores were depleted. Atazanavir and indinavir had similar effects on ER calcium stores (data not shown).

Effects of HIV PIs on SREBPs in Macrophages. SREBPs play critical roles in lipid homeostasis and directly activate the expression of dozens of genes involved in lipid metabolism. SREBP-1 is primarily involved in regulating fatty acid and triglyceride biosynthesis, whereas SREBP-2 is involved in sterol biosynthesis and metabolism. It has been reported that HIV PIs cause severe hyperlipidemia and lipodystrophy in some patients (Friis-Moller et al., 2003; Hui, 2003; Fontas et al., 2004). Our previous studies showed that indinavir increased the levels of activated SREBP-1 and SREBP-2 in rat hepatocytes (Williams et al., 2004). To examine the effect of HIV PIs on the expression of SREBPs in mouse J774A.1 macrophages, cells were treated with HIV PIs (ritonavir, indinavir, and atazanavir) at therapeutic concentration (15 μM) for various times. The levels of transcriptionally active mature SREBP-1 and SREBP-2 were significantly increased as shown in Fig. 6. Treatment of these cells with ritonavir (15 μM) for 6 h, increased the levels of mature SREBP-1 and SREBP-2 by 273% and 82% ($p < 0.05$), respectively. This HIV PI also increased the level of the precursor form of SREBP-1 (data not shown).

Effects of Ritonavir on Free Cholesterol Accumulation and Esterification in Macrophages. Maintenance of the cellular cholesterol homeostasis is crucial to various cellular functions. To further define whether HIV PI-induced activation of SREBPs is associated with a corresponding increase in intracellular free cholesterol, mouse macrophages

Fig. 4. Ritonavir induces apoptosis and activates caspase-12 in mouse J774A.1 macrophages. Cells were treated with vehicle control or various concentrations of ritonavir (5–50 μM) for 24 h, then stained with Annexin V-FITC/propidium iodide. A, images of Annexin V/propidium iodide-stained cells were visualized under confocal fluorescence microscope with a dual filter set for FITC and rhodamine. B, the percentages of apoptotic cells were analyzed by flow cytometry. The results are the mean ± S.E. for three independent experiments. *, statistical significance relative to vehicle control, $p < 0.05$. C, activity of caspase-12 in whole-cell lysates of mouse J774A.1 macrophages treated with ritonavir (0–25 μM) or thapsigargin (100 nM) for 24 h was measured using Caspase-12 Fluorometric assay kit according to the manufacturer's instruction. *, statistical significance relative to vehicle control, $p < 0.05$.

were treated with different concentrations of ritonavir (5–50 μM) for 24 h, and the free cholesterol was detected with filipin staining. As shown in Fig. 7A, ritonavir modestly induced the accumulation of free cholesterol in intracellular membranes of mouse macrophages. Treatment with 15 to 25 μM ritonavir increased intracellular free cholesterol content (Fig. 7B). However, treatment with thapsigargin (100 nM) for 24 h did not cause the accumulation of free cholesterol in macrophage (Fig. 7, A and B). These results indicate that activation of UPR is not the direct cause of the HIV PI-induced free cholesterol accumulation in mouse macrophages. We were surprised to find that even though intracellular cholesterol levels increased, there was a significant decrease in endogenous cholesterol esterification (Fig. 7C). In contrast, exogenous cholesterol esterification was not affected (Fig. 7D). The amount of total esterified cholesterol was not affected by ritonavir (Fig. 7B).

Effects of Ritonavir on the Expression of ABCA1, ABCG1, CD36, and LDLR in Macrophages. To determine whether HIV PIs regulate the genes related to cholesterol uptake and efflux, such as LDLR, CD36, ABCA1, and ABCG1, we used quantitative PCR to measure the mRNA level of these receptors and lipid transporters in control and ritonavir-treated cells. Mouse J774A.1 cells were treated with ritonavir (15 μM), thapsigargin (100 nM), or control vehicle for 24 h, and total RNA was isolated. The mRNA levels of ABCA1, ABCG1, LDLR, and CD 36 were quantified using specific gene expression assay kits. The results (Table 1) show that ritonavir had no effect on mRNA levels of ABCA1 and ABCG1, but significantly increased CD36 and

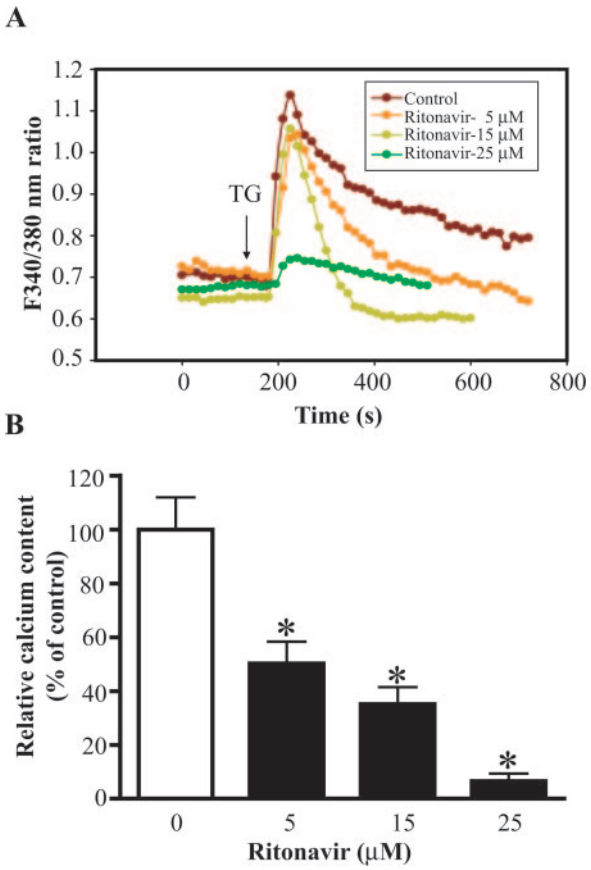

Fig. 5. Depletion of endoplasmic reticulum calcium stores by ritonavir. A, assessment of endoplasmic reticulum calcium stores in mouse J774A.1 macrophages treated for 24 h with different concentrations of ritonavir (0, 5, 15, and 25 μM). Representative tracings of the Fura-2 fluorescence ratio of 340:380 nm in an individual macrophage for each treatment group before and after addition of 100 nM thapsigargin are shown. B, relative calcium content was calculated by total area under the curve for each treatment group and expressed as a percentage of vehicle control. *, statistical significance relative to vehicle control, $p < 0.05$.

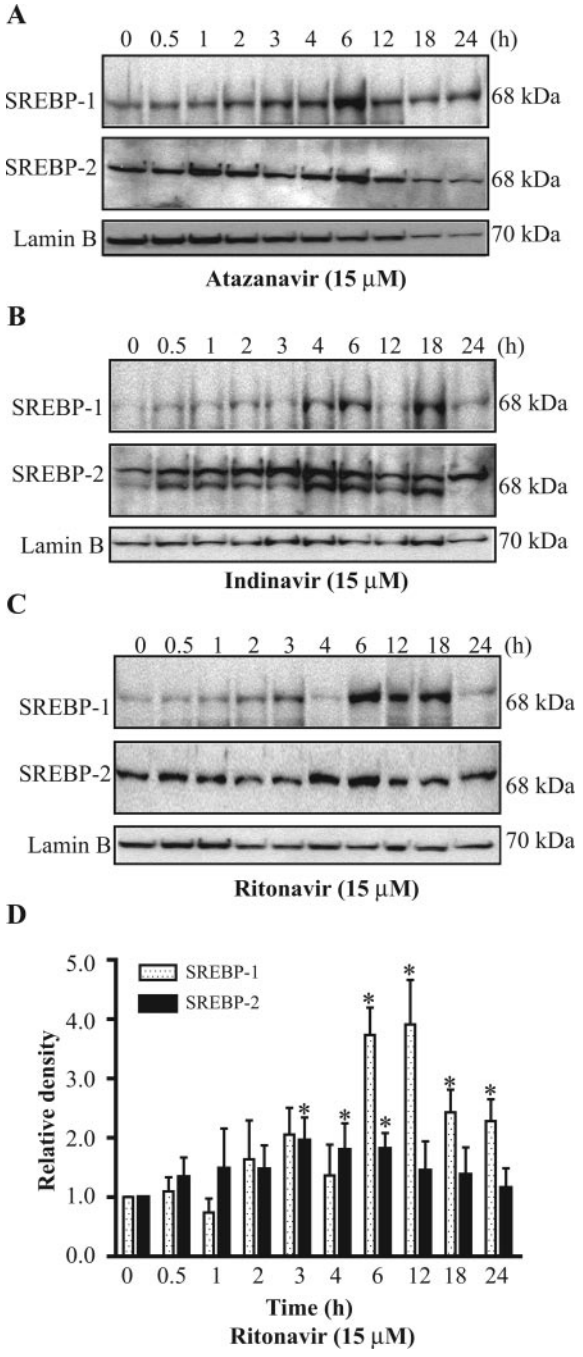

Fig. 6. Time course of the HIV PI-induced activation of SREBP-1 and SREBP-2. Representative immunoblots against SREBP-1, SREBP-2, and lamin B from the nuclear extracts of mouse J774A.1 macrophages treated with HIV PIs (15 μM) for 0, 0.5, 1, 2, 3, 4, 6, 12, 18, and 24 h. Lamin B was used as a loading control. Atazanavir (A), indinavir (B), ritonavir (C), and relative density of the immunoblots against SREBP-1 and SREBP-2 activated by ritonavir (D). The density of the immunoreactive bands was analyzed using Image J software and normalized to lamin B control. Values are mean ± S.E. of three independent experiments. *, statistical significance relative to vehicle control, $p < 0.05$.

LDLR mRNA levels. However, thapsigargin, a positive control of ER stress inducer, significantly decreased CD36 mRNA level and had little effect on ABCA1, ABCG1, and LDLR mRNA levels.

Ritonavir Activated the UPR and Induced Apoptosis in Foam Cells. Lipid-laden macrophages (foam cells) are found in all stages of atherosclerosis. Unstable human atherosclerotic plaques constitute numerous foam cells. Apoptosis of foam cells is extremely detrimental. To further examine whether HIV PIs can also induce ER stress, activate the UPR, and increase apoptosis in foam cells, mouse J774A.1 cells were loaded with Ac-LDL (50 μg/ml) or vehicle control for 24 h and then treated with ritonavir (15 μM), thapsigargin (100 nM), or vehicle for 24 h. The intracellular lipids were

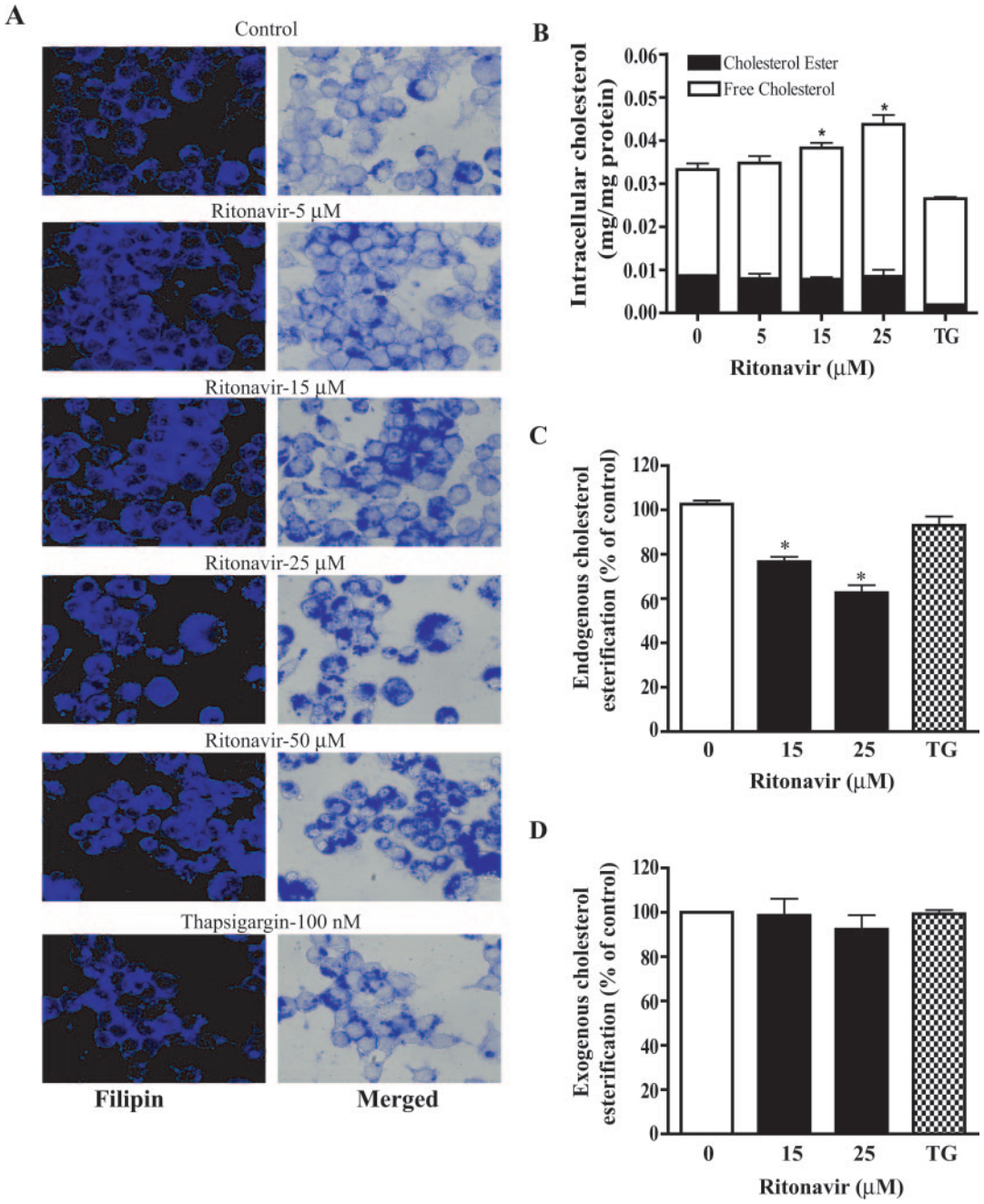

Fig. 7. Effects of ritonavir on the accumulation of free cholesterol in mouse J774A.1 macrophages and cholesterol esterification. A, cells were treated with various concentrations of ritonavir (0–50 μM) or thapsigargin (100 nM) for 24 h and stained with Filipin for free cholesterol as described under *Materials and Methods*. Fluorescence images and merged phase-contrast images are shown. B, cells were treated with various concentrations of ritonavir (0–25 μM) or thapsigargin (100 nM) for 24 h. The intracellular total and free cholesterol contents were measured using Wako Cholesterol E and Free Cholesterol assay kits. Values are mean ± S.E. of three independent experiments. *, statistical significance relative to vehicle control, $p < 0.05$. C, endogenous cholesterol esterification. Cells were treated with ritonavir (15 and 25 μM) for 24 h in LDL-deficient medium and labeled with [^{3}H]oleate. The [^{3}H]cholesteryl oleate was analyzed and quantified as described under *Materials and Methods*. Data are expressed as a percentage of control vehicle, and values are mean ± S.E. of three independent experiments. *, statistical significance relative to vehicle control, $p < 0.05$. D, exogenous cholesterol esterification. Cells were treated with ritonavir (15 and 25 μM) for 24 h in LDL-containing medium and labeled with [^{3}H]oleate. The [^{3}H]cholesteryl oleate was analyzed and quantified as described under *Materials and Methods*. Data are expressed as a percentage of control vehicle and values are mean ± S.E. of three independent experiments. *, statistical significance relative to vehicle control, $p < 0.05$.

stained with oil red O. The expression of CHOP, ATF-4, and XBP-1 were detected by Western blot; the apoptotic cells were detected by Annexin V-FITC/propidium iodide staining with confocal fluorescence microscopy. As shown in Fig. 8, A and B, ritonavir increased the lipid accumulation not only in Ac-LDL–loaded cells but also in normal macrophages, suggesting that ritonavir may promote the foam cell formation. In Ac-LDL–induced foam cells, ritonavir modestly increased the accumulation of the intracellular free cholesterol, but significantly increased cholesterol ester accumulation (Fig. 8C). Treatment of foam cells with ritonavir (0–50 μM) induced dose-dependent apoptosis. As shown in Fig. 9, Ac-LDL–induced foam cells were more sensitive to ritonavir compared with normal cholesterol loaded macrophages. Likewise, ritonavir activated the UPR in foam cells (Fig. 10).

Discussion

Clinical studies report that HIV PIs increase serum lipids (Hui, 2003), promote atherosclerosis (Sklar and Masur, 2003), and increase the risk of myocardial infarction (Friis-Moller et al., 2003) in patients with HIV infection. Studies using rodent macrophages (Dressman et al., 2003) and hepatocytes (Liang et al., 2001; Riddle et al., 2001) have shown that HIV PIs dysregulate cellular lipid metabolism. However, the exact mechanism(s) altering lipid metabolism is unclear and may be multifactorial. Our current studies show that HIV PIs (ritonavir, indinavir, and atazanavir) activate the UPR and induce apoptosis in both normal cholesterol loaded macrophages and in Ac-LDL–loaded macrophages. We were surprised to find that HIV PIs markedly increased the mature forms of nuclear SREBP-1 and SREBP-2 (Fig. 6) and increased cholesterol in intracellular membranes (Fig. 7). HIV PI-induced disruption of lipid homeostasis and enhanced programmed cell death occurred in macrophages at concentrations (5–15 μM) that are within serum levels reported for patients infected with HIV who are taking these medications (Flexner, 1998).

In mammalian cells, the ER is involved in the proper folding and post-translational modification of proteins. The ER also maintains very low membrane cholesterol content (Feng et al., 2003) and is very sensitive to alterations in cellular homeostatic mechanisms. A number of cellular stress conditions can alter the normal rate of folding and processing of newly synthesized proteins (Pahl, 1999). The ER has evolved cell signaling pathways to respond to the accumulation of unfolded or misfolded proteins, collectively referred to as the UPR (reviewed in Zhang and Kaufman, 2004). Activation of the UPR allows mammalian cells to increase protein folding and degradation pathways and differentially inhibits most protein synthesis. However, prolonged activation of the UPR can lead to apoptosis.

Macrophages are the major cell type found in atherosclerotic lesions, and inappropriate and/or excessive apoptosis of these cells is believed to play a key role in both the initiation and the progression of atherosclerosis. Compounds that activate the UPR in vivo seem to accelerate cardiovascular disease. For example, patients with hyperhomocystinemia

TABLE 1

Effect of ritonavir on the mRNA levels of ABCA1, ABCG1, CD36, and LDLR in mouse J774A.1 macrophages

Mouse J774A.1 cells were treated with ritonavir (15 μM), thapsigargin (100 nM), or vehicle control for 24 h. Total cellular RNA was isolated using Ambion RNAqueous kit and used for first-strand cDNA synthesis using the High-Capacity cDNA archive kit. The mRNA levels of ABCA1, ABCG1, CD36, and LDLR were quantified using the specific gene expression assay kits for mouse ABCA1, ABCG1, CD36, and LDLR on an ABI PRISM7700 Sequence Detection System. The mRNA values for each gene were normalized to internal control β-actin mRNA. The ratio of normalized mean value for each treatment groups to vehicle control was calculated. The values are mean ± S.E. of three independent experiments.

Treatment	Gene			
	ABCA1	ABCG1	CD36	LDLR
Control	1.16 ± 0.27	1.02 ± 0.067	1.10 ± 0.11	1.10 ± 0.24
Ritonavir,15 μM	1.63 ± 0.56	1.30 ± 0.11	2.75 ± 0.36*	3.80 ± 0.26*
Thapsigargin,100 nM	1.18 ± 0.33	0.70 ± 0.18	0.40 ± 0.06*	1.64 ± 0.09

* $p < 0.05$, statistical significance relative to vehicle control.

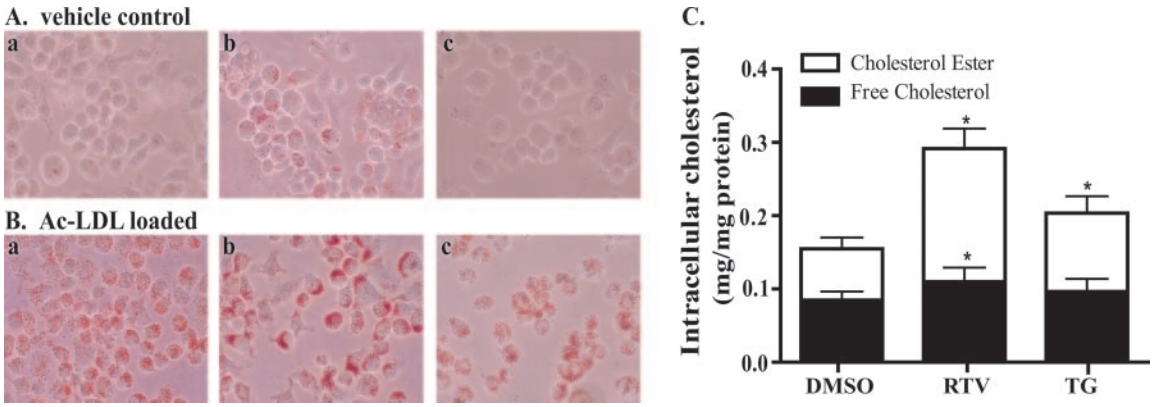

Fig. 8. Effects of ritonavir on intracellular cholesterol and lipid content in macrophages. Normal mouse J774A.1 macrophages (A) or Ac-LDL loaded (50 μg/ml for 24 h) macrophages (B) were treated with vehicle control (a), ritonavir (15 μM) (b), or thapsigargin (100 nM) (c) for 24 h. The intracellular lipids were stained with 0.2% oil red O as described under *Materials and Methods*. The images were taken with the use of an Olympus microscope equipped with an image recorder. C, Ac-LDL–loaded macrophages were treated with vehicle control [dimethyl sulfoxide (DMSO)], ritonavir (RTV, 15 μM), or thapsigargin (TG, 100 nM) for 24 h. The intracellular total and free cholesterol contents were measured using Wako Cholesterol E and Free Cholesterol assay kits. Values are mean ± S.E. of three independent experiments. *, statistical significance relative to vehicle control, $p < 0.05$.

accumulate high serum levels of homocysteine because of genetic defects in genes involved in homocysteine metabolism (Outinen et al., 1999). Hyperhomocystinemia is an independent risk factor for atherosclerosis and cardiovascular disease. Homocysteine has been shown to be an activator of the UPR in hepatocytes and vascular endothelial cells (Werstuck et al., 2001). Activation of the UPR by homocysteine is associated with dysregulation of lipid metabolism, increased apoptosis, and accelerated atherosclerosis. We hypothesize that HIV PIs accelerate atherosclerosis and cardiovascular disease as a result of their ability to disrupt normal lipid metabolism and to activate the UPR.

It is currently unclear how HIV protease inhibitors activate the UPR; a number of cellular stress signals, such as depletion of ER calcium stores, increased cholesterol in ER membranes, deprivation of glucose (Oyadomari and Mori, 2004), or inhibition of proteasome activity (Parker et al., 2005) can activate this system. Recent studies have shown that overloading of free cholesterol in the ER causes depletion of ER calcium stores (by inhibiting the sarcoplasmic-endoplasmic reticulum calcium ATPase-2b) (Li et al., 2004), activates the UPR, and induces apoptosis in macrophages (Feng et al., 2003). In the present study, we discovered that HIV PIs induced accumulation of free cholesterol and lipid in intracellular membranes of mouse macrophages and depleted ER calcium stores (as shown in Figs. 5; 7, A and B; and 8). However, there was no direct effect of HIV PIs on ER calcium release (data not shown). Therefore, one possible mechanism by which HIV PIs activate the UPR in macrophages is the accumulation of intracellular free cholesterol followed by the depletion of ER calcium stores.

Macrophages have acquired multiple mechanisms to prevent the accumulation of excess free cholesterol, including an increase in cholesterol esterification, induction of free cholesterol efflux, and down-regulation of cholesterol biosynthesis (Zhang and Kaufman, 2003). HIV PIs may promote foam cell formation and atherosclerosis by modulation of CD36 (Dressman et al., 2003) and the LDLR (Tran et al., 2003) and by increasing cholesterol biosynthesis. In the present study, we demonstrated that ritonavir significantly up-regulates CD36 and LDLR mRNA expression but has no effect on ABCA1 and ABCG1 mRNA levels. It has been demonstrated that overloading of free cholesterol in macrophages decreases ABCA1-mediated cholesterol efflux by accelerating the degradation of ABCA1 protein (Feng and Tabas, 2002). Thus, HIV PI-induced accumulation of intracellular free cholesterol and lipid may indirectly impair the normal function of ABCA1 protein. It has also been shown that disruption of intracellular cholesterol transport may adversely affect cholesterol efflux and cholesterol esterification (Tabas, 2002).

It has been reported that depletion of glucose causes the accumulation of unfolded proteins, induces ER stress, and activates the UPR (Pahl, 1999). It has been demonstrated that indinavir selectively and reversibly inhibits the glucose transporter isoform GluT4 at therapeutic concentrations (Murata et al., 2002; Koster et al., 2003) and impairs SREBP-1 intranuclear localization (Caron et al., 2001). These observations suggest another possible mechanism by which HIV PIs might induce ER stress and activate the UPR.

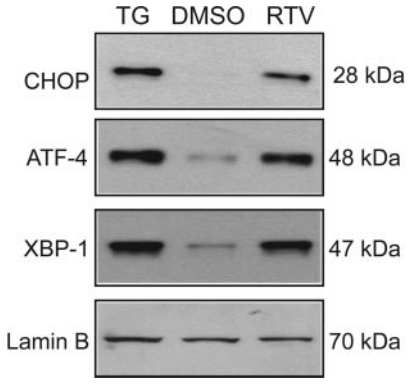

Fig. 10. Activation of the UPR by ritonavir in Ac-LDL–loaded macrophages. Representative immunoblots against CHOP, ATF-4, XBP-1, and lamin B from the nuclear extracts of mouse macrophages loaded with Ac-LDL (50 μg/ml) and treated with ritonavir (RTV, 15 μM) for 24 h. Lamin B was used as a loading control. Thapsigargin (TG, 100 nM) was used as a positive control. Dimethyl sulfoxide (DMSO) was the vehicle control.

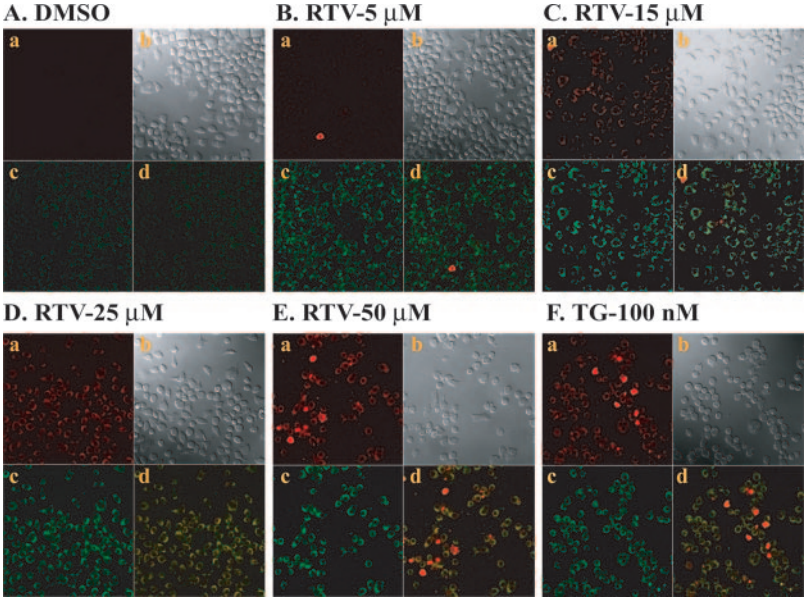

Fig. 9. Ritonavir induces apoptosis of Ac-LDL–loaded cells (foam cells). Mouse macrophages were loaded with Ac-LDL (50 μg/ml) for 24 h then treated with different concentrations of ritonavir (RTV, 0–50 μM) or thapsigargin (TG, 100 nM) for 24 h. Apoptotic cells were stained with Annexin V-FITC/propidium iodide and visualized with a dual filter set for FITC and rhodamine. a, propidium iodide staining; b, phase contrast image; c, annexin V-FITC staining; and d, FITC and propidium iodide-merged images.

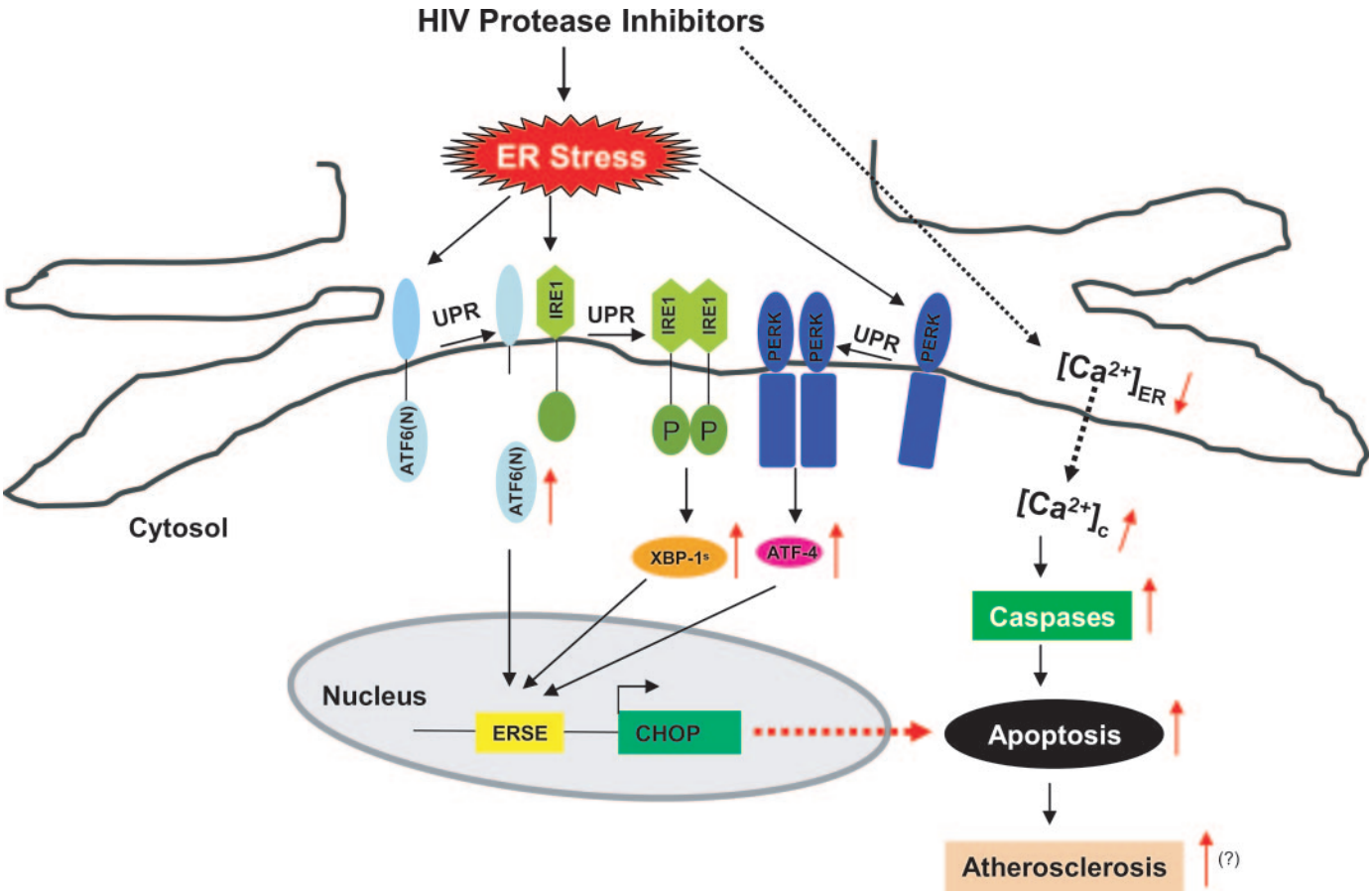

Fig. 11. Proposed model of HIV PI-induced UPR signaling pathways in macrophages. HIV PIs induce ER stress and activate the UPR in macrophages. Activation of ATF-4, XBP-1, and ATF-6 results in transcriptional induction of the CHOP gene. HIV PIs also increase cytosolic calcium and activate caspase-12. Both CHOP and caspase-12 mediate ER stress-induced apoptosis. IRE1, inositol-requiring enzyme, a transmembrane protein kinase/endoribonuclease; PERK, doubled-stranded RNA-activated protein kinase-like ER kinase; ERSE, ER stress response element. CHOP is also called GADD153 (growth arrest and DNA damage-inducing gene).

However, whether HIV PIs disrupt glucose homeostasis in macrophages needs further investigation.

Most recent studies done by Parker et al. (2005) suggest that inhibition of proteasome activity and differential glucose transport by HIV PIs are proximal events eliciting the UPR, which can regulate lipogenic pathways in hepatocytes or adipocytes. Several studies have shown that ritonavir is a reversible inhibitor of proteasome and inhibits the chymotrypsin-like activity of the proteasome while enhancing the trypsin-like activity at high concentration (50–100 μM) (Lagathu et al., 2004; Laurent et al., 2004). However, a block in proteasomal housekeeping functions in intact cells by ritonavir requires 50 to 100 μM concentrations of the drug (Andre et al., 1998). In the present studies, the UPR is activated by ritonavir at concentrations (5–15 μM) at which essential functions of the proteasome are not yet blocked. In vitro studies have also shown that different HIV PIs differ in their effects on proteasome activity. Indinavir and nelfinavir have no effect on proteasome activity even at high concentration (100 μM) (Andre et al., 1998). However, in our studies, we observed that indinavir induced the UPR activation and disrupted lipid metabolism at clinically relevant concentration (15 μM) in macrophages. Nelfinavir is also able to induce the UPR activation at even lower concentrations (1–10 μM) (unpublished data). Therefore, the HIV PI-induced activation of the UPR may not be due to the dysfunction of the proteasome in macrophages.

In summary, the current study provides novel insights into how HIV PIs induce ER stress, activate the UPR, and induce apoptosis in macrophages (Fig. 11). The effects of HIV PIs on accumulation of intracellular free cholesterol and lipids and depletion of ER calcium stores represent a potential mechanism by which HIV PIs induce atherosclerosis and cardiovascular disease in patients infected with HIV who are undergoing HARRT. Different HIV PIs have different effects in different cell types. We cannot rule out the involvement of other target proteins in the HIV PI-induced activation of the UPR and apoptosis in macrophages. A better understanding of the cellular and molecular mechanisms of HIV PI-induced metabolic abnormality may provide useful information for the development of new drugs and therapeutic strategies.

Acknowledgments

We thank Abbott Laboratories (ritonavir), Merck & Co., Inc. (indinavir), and Bristol-Meyers-Squibb (atazanavir) for providing us with the compounds used in this research.

References

Andre P, Groettrup M, Klenerman P, de Giuli R, Booth BL Jr, Cerundolo V, Bonneville M, Jotereau F, Zinkernagel RM, and Lotteau V (1998) An inhibitor of HIV-1

protease modulates proteasome activity, antigen presentation and T cell responses. *Proc Natl Acad Sci USA* **95:**13120–13124.
Beregszaszi M, Jaquet D, Levine M, Ortega-Rodriguez E, Baltakse V, Polak M, and Levy-Marchal C (2003) Severe insulin resistance contrasting with mild anthropometric changes in the adipose tissue of HIV-infected children with lipohypertrophy. *Int J Obes Relat Metab Disord* **27:**25–30.
Bongiovanni M, Bini T, Chiesa E, Cicconi P, Adorni F, and Monforte d A (2004) Lopinavir/ritonavir vs. Indinavir/ritonavir in antiretroviral naive HIV-infected patients: immunovirological outcome and side effects. *Antiviral Res* **62:**53–56.
Caron M, Auclair M, Vigouroux C, Glorian M, Forest C, and Capeau J (2001) The HIV protease inhibitor indinavir impairs sterol regulatory element-binding protein-1 intranuclear localization, inhibits preadipocyte differentiation and induces insulin resistance. *Diabetes* **50:**1378–1388.
Carr A, Samaras K, Burton S, Law M, Freund J, Chisholm DJ, and Cooper DA (1998) A syndrome of peripheral lipodystrophy, hyperlipidaemia and insulin resistance in patients receiving HIV protease inhibitors. *AIDS* 12:F51–F58.
Dressman J, Kincer J, Matveev SV, Guo L, Greenberg RN, Guerin T, Meade D, Li XA, Zhu W, Uittenbogaard A, et al. (2003) HIV protease inhibitors promote atherosclerotic lesion formation independent of dyslipidemia by increasing CD36-dependent cholesteryl ester accumulation in macrophages. *J Clin Investig* **111:** 389–397.
Feng B and Tabas I (2002) ABCA1-mediated cholesterol efflux is defective in free cholesterol-loaded macrophages. Mechanism involves enhanced ABCA1 degradation in a process requiring full NPC1 activity. *J Biol Chem* **277:**43271–43280.
Feng B, Yao PM, Li Y, Devlin CM, Zhang D, Harding HP, Sweeney M, Rong JX, Kuriakose G, Fisher EA, et al. (2003) The endoplasmic reticulum is the site of cholesterol-induced cytotoxicity in macrophages. *Nat Cell Biol* **5:**781–792.
Flexner C (1998) HIV-protease inhibitors. *N Engl J Med* **338:**1281–1292.
Fontas E, van LF, Sabin CA, Friis-Moller N, Rickenbach M, d'Arminio MA, Kirk O, Dupon M, Morfeldt L, Mateu S, et al. (2004) Lipid profiles in HIV-infected patients receiving combination antiretroviral therapy: are different antiretroviral drugs associated with different lipid profiles? *J Infect Dis* **189:**1056–1074.
Friis-Moller N, Sabin CA, Weber R, d'Arminio Monforte A, El-Sadr WM, Reiss P, Thiebaut R, Morfeldt L, De Wit S, Pradier C, et al. (2003) Combination antiretroviral therapy and the risk of myocardial infarction. *N Engl J Med* **349:**1993–2003.
Holmberg SD, Moorman AC, Greenberg AE (2004) Trends in rates of myocardial infarction among patients with HIV. *N Engl J Med* **350:**730–732.
Horton JD, Goldstein JL, and Brown MS (2002) SREBPs: activators of the complete program of cholesterol and fatty acid synthesis in the liver. *J Clin Investig* **109:**1125–1131.
Hui DY (2003) Effects of HIV protease inhibitor therapy on lipid metabolism. *Prog Lipid Res* **42:**81–92.
Koster JC, Remedi MS, Qiu H, Nichols CG, and Hruz PW (2003) HIV protease inhibitors acutely impair glucose-stimulated insulin release. *Diabetes* **52:**1695–1700.
Lagathu C, Bastard JP, Auclair M, Maachi M, Kornprobst M, Capeau J, and Caron M (2004) Antiretroviral drugs with adverse effects on adipocyte lipid metabolism and survival alter the expression and secretion of proinflammatory cytokines and adiponectin in vitro. *Antivir Ther* **9:**911–920.
Laurent N, de Bouard S, Guillamo JS, Christov C, Zini R, Jouault H, Andre P, Lotteau V, Peschanski M (2004) Effects of the proteasome inhibitor ritonavir on glioma growth in vitro and in vivo. *Mol Cancer Ther* **3:**129–136.
Li Y, Ge M, Ciani L, Kuriakose G, Westover EJ, Dura M, Covey DF, Freed JH, Maxfield FR, Lytton J, et al. (2004) Enrichment of endoplasmic reticulum with cholesterol inhibits sarcoplasmic-endoplasmic reticulum calcium ATPase-2b activity in parallel with increased order of membrane lipids: implications for depletion of endoplasmic reticulum calcium stores and apoptosis in cholesterol-loaded macrophages. *J Biol Chem* **279:**37030–37039.
Liang JS, Distler O, Cooper DA, Jamil H, Deckelbaum RJ, Ginsberg HN, and Sturley SL (2001) HIV Protease inhibitors protect apolipoprotein B from degradation by the proteasome: a potential mechanism for protease inhibitor-induced hyperlipidemia. *Nat Med* **7:**1327–1331.
Murata H, Hruz PW, and Mueckler M (2002) Indinavir inhibits the glucose transporter isoform Glut4 at physiologic concentrations. *AIDS* **16:**859–863.
Nakagawa T, Zhu H, Morishima N, Li E, Xu J, Yankner BA, and Yuan J (2000) Caspase-12 mediates endoplasmic-reticulum-specific apoptosis and cytotoxicity by amyloid-beta. *Nature (Lond)* **403:**98–103.
Outinen PA, Sood SK, Pfeifer SI, Pamidi S, Podor TJ, Li J, Weitz JI, and Austin RC (1999) Homocysteine-induced endoplasmic reticulum stress and growth arrest leads to specific changes in gene expression in human vascular endothelial cells. *Blood* **94:**959–967.
Oyadomari S and Mori M (2004) Roles of CHOP/GADD153 in endoplasmic reticulum stress. *Cell Death Differ* **11:**381–389.
Pahl HL (1999) Signal transduction from the endoplasmic reticulum to the cell nucleus. *Physiol Rev* **79:**683–701.
Parker RA, Flint OP, Mulvey R, Elosua C, Wang F, Fenderson W, Wang S, Yang WP, Noor MA (2005) Endoplasmic reticulum stress links dyslipidemia to inhibition of proteasome activity and glucose transport by HIV protease inhibitors. *Mol Pharmacol* **67:**1909–1919.
Riddle TM, Kuhel DG, Woollett LA, Fichtenbaum CJ, and Hui DY (2001) HIV protease inhibitor induces fatty acid and sterol biosynthesis in liver and adipose tissues due to the accumulation of activated sterol regulatory element-binding proteins in the nucleus. *J Biol Chem* **276:**37514–37519.
Rutkowski DT and Kaufman RJ (2004) A trip to the ER: coping with stress. *Trends Cell Biol* **14:**20–28.
Sklar P and Masur H (2003) HIV infection and cardiovascular disease—is there really a link? *N Engl J Med* **349:**2065–2067.
Stanley ER, Cifone M, Heard PM, and Defendi V (1976) Factors regulating macrophage production and growth: identity of colony-stimulating factor and macrophage growth factor. *J Exp Med* **143:**631–647.
Tabas I (2002) Consequences of cellular cholesterol accumulation: basic concepts and physiological implications. *J Clin Investig* **110:**905–911.
Tabas I (2004) Apoptosis and plaque destabilization in atherosclerosis: the role of macrophage apoptosis induced by cholesterol. *Cell Death Differ* **11 (Suppl 1):**S12–S16.
Tran H, Robinson S, Mikhailenko I, and Strickland DK (2003) Modulation of the LDL receptor and LRP levels by HIV protease inhibitors. *J Lipid Res* **44:**1859–1869.
Werstuck GH, Lentz SR, Dayal S, Hossain GS, Sood SK, Shi YY, Zhou J, Maeda N, Krisans SK, Malinow MR, et al. (2001) Homocysteine-induced endoplasmic reticulum stress causes dysregulation of the cholesterol and triglyceride biosynthetic pathways. *J Clin Investig* **107:**1263–1273.
Williams K, Rao YP, Natarajan R, Pandak WM, and Hylemon PB (2004) Indinavir alters sterol and fatty acid homeostatic mechanisms in primary rat hepatocytes by increasing levels of activated sterol regulatory element-binding proteins and decreasing cholesterol 7alpha-hydroxylase MRNA levels. *Biochem Pharmacol* **67:** 255–267.
Yamaguchi H and Wang HG (2004) CHOP is involved in endoplasmic reticulum stress-induced apoptosis by enhancing DR5 expression in human carcinoma cells. *J Biol Chem* **279:**45495–45502.
Zhang K and Kaufman RJ (2003) Unfolding the toxicity of cholesterol. *Nat Cell Biol* **5:**769–770.
Zhang K and Kaufman RJ (2004) Signaling the unfolded protein response from the endoplasmic reticulum. *J Biol Chem* **279:**25935–25938.

Address correspondence to: Dr. Phillip B. Hylemon, Department of Microbiology and Immunology, Virginia Commonwealth University, P.O. Box 980678, Richmond, VA 23298-0678. E-mail: hylemon@hsc.vcu.edu